

# Optimization of sound-absorbing material ratio and sound field simulation for indoor acoustic environmental art design

Qing Guo<sup>1,\*</sup>

<sup>1</sup> School of Fine Arts, ZhengZhou Vocational College of Finance and Taxation, Zhengzhou, Henan, 450000, China

Corresponding authors: (e-mail: g23455758@163.com).

**Abstract** This paper constructs a simulation model of indoor sound field based on ODEON software, and proposes an iterative updating strategy for the distribution of sound-absorbing materials in combination with the topology optimization algorithm. Combined with 2D boundary element model and finite element analysis, the validity of sound field simulation and optimization effect of sound-absorbing materials are verified. Through the 2D boundary element model and the sound barrier optimization case, it is verified that the reverberation time of each room is adjusted under the effect of room coupling, and the difference between the reverberation time of the master bedroom and the living room under the same frequency is not more than 0.05 s. The optimized material has a surface density of 0.39 kg/m<sup>2</sup>, which has the largest sound absorption coefficient, and it has a very good acoustic absorption effect for the mid-frequency band as well. In order to achieve the same acoustic effect, glass fiber acoustic cotton needs to be 80mm thick. The results highlight the importance of optimizing the design of the ratio of sound-absorbing materials.

**Index Terms** ODEON, topology optimization, 2D boundary element model, sound field simulation, sound absorbing material

## I. Introduction

Acoustic design is based on the principle of acoustics, which covers the knowledge of sound generation, propagation and reception [1]. In the indoor art environment, acoustic design can achieve good acoustic effect through reasonable layout of sound sources, selection of sound-absorbing materials and noise control [2], [3]. And indoor acoustic environment art design is an important work to ensure that the transmission and reflection of sound in the indoor space to achieve the best effect, which includes sound wave propagation, reflection, absorption, etc., and a good indoor acoustic environment can improve the quality of people's lives and work efficiency inside the building, which needs to be considered in a comprehensive manner of the ratio of the sound-absorbing materials [4]-[7].

The first task of architectural acoustic environment art design is to understand the propagation characteristics of sound waves [8]. When sound waves propagate in different materials and spatial shapes, they are affected by a variety of factors, so the selection of sound-absorbing materials and the optimization of ratios are crucial [9], [10]. The design of sound-absorbing materials and the improvement of acoustic environment are an interdependent process [11]. Through scientific design of sound-absorbing materials, the acoustic environment can be effectively improved and the interference of noise and echo can be reduced [12]. Therefore, when selecting sound-absorbing materials, they need to be customized according to the acoustic characteristics and needs of the place in order to achieve the desired acoustic effect [13], [14]. Meanwhile, the evaluation of the effect of acoustic environment improvement can help us to judge the effectiveness of sound-absorbing materials and optimize and improve them [15], [16]. Designers need to select appropriate materials according to the functional requirements of the space to achieve the best indoor acoustic environment [17].

This paper firstly briefly introduces the application of ODEON in building acoustic design, and systematically combs through the algorithm and function overview of ODEON software. Based on the variable density topology optimization method of the isotropic penalized microstructure model method, the relative density of the acoustic absorption material unit is taken as the design variable. The volume of the sound-absorbing material is used as the constraint, and the lowest sound pressure value at the reference surface is used as the design objective to construct the topology optimization mathematical model. The sensitivity calculation is performed using the boundary element method, and the optimization model is solved using the moving asymptote optimization algorithm. A two-dimensional boundary element model is used to study the acoustic diffusivity of the apartment, and the model is validated by Morse's simple positive theory using rigid and soft boundary conditions. The acoustic diffusion equation is applied

to the finite element simulation of coupled indoor acoustics to explore the effect of acoustic structure on the spatial distribution of sound pressure level. The simplified model of glass fiber acoustic cotton is selected as the optimization object to verify the feasibility of the topology optimization method proposed in this paper.

## II. ODEON-based sound field simulation for indoor acoustic environment

### II. A. Application of ODEON in building acoustics

The mainstream sound field simulation software on the market at present are EASE, ODEON and RAYNOISE, etc., which are all applied in the design, consultation and research of building acoustics. ODEON, which is used in the experiments of this paper, adopts the method of combining simulated sound source and sound line tracking based on the principle of physical acoustics for sound field simulation, which can be applied to the design of hall acoustics, arena acoustics and noise control.

To simulate and analyze the indoor sound field with ODEON, it is necessary to establish a three-dimensional model of the hall firstly, and the three-dimensional model can be realized by the modeling language embedded in ODEON or by the software such as AutoCAD which is converted into the file format acceptable to ODEON; ODEON will then check the sealing of the three-dimensional model and prompt the user to make corrections; the model should be set up in accordance with the actual situation after it passes the checking. ODEON has a database of sound-absorbing materials and simulated sound sources, which can be added and modified by the user as appropriate. The flow of ODEON modeling for sound field simulation is shown in Figure 1.

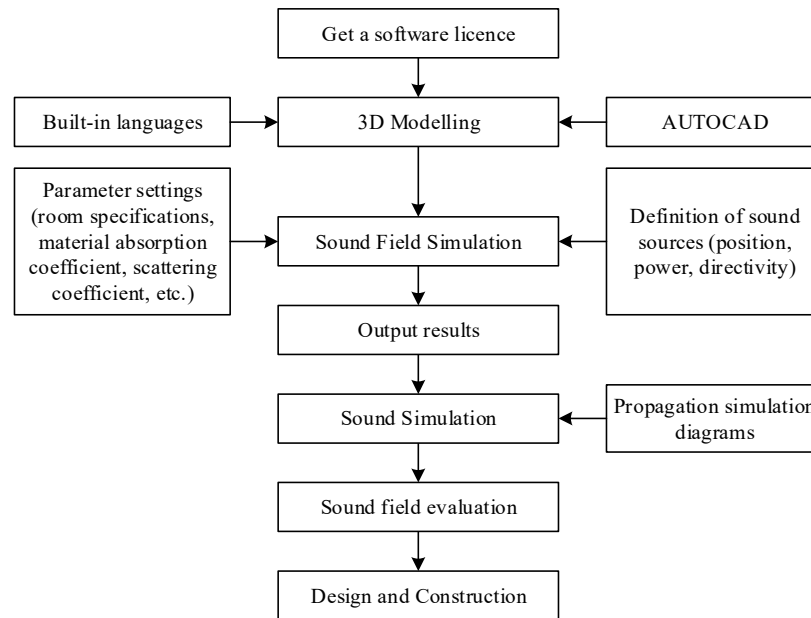


Figure 1: The flow of ODEON modeling for sound field simulation

The indoor sound quality parameters calculated by ODEON are based on the ISO 3382 standard and contain measurable indoor acoustic parameters, including early decay time EDT, reverberation time T30, clarity C80, definition D50, time center of gravity Ts, lateral energy factor LF, sound field strength G and speech transmission index STI. As an aid to sound quality design, ODEON calculates a sequence diagram of the reflected sound at each reception point, giving not only the time and energy of the arrival of the reflected sound, but also the direction of the path of the reflected sound and the participating surfaces (sound tracking), which is intuitive for eliminating or correcting specific reflections, determining echoes and other issues.

ODEON has an audible module that makes it possible to hear the desired sound effects at the design stage. The principle is to calculate the binaural room impulse response (BRIR) at certain points in the hall to obtain a pair of impulse response signals, and then convolve the “dry” signals recorded in the anechoic chamber (which can be speech, music, or other signals relevant to the listening test) with these pairs of impulse response signals, to obtain an audible signal of the sound quality under the relevant conditions, all in one step. The entire process is completed in one step, without post-processing, and ODEON comes with a number of anechoic chamber recordings that can be added or subtracted by the user.

## II. B. Overview of the algorithms and functions of the ODEON software

### II. B. 1) Overview of computer simulation of indoor sound fields

Indoor sound field simulation technology is based on geometric acoustics, the propagation of sound waves and energy attenuation process is described by a large number of sound lines emitted by the source or the source of the reflection interface into the various times the sound image, which gives rise to two classic simulation methods: the sound line method and the sound image method.

#### (1) Line-of-sound method

The sound line method assumes that a large number of sound particles propagating in different directions are emitted from the sound source, and the sound particles collide with the interface, changing both the energy and the direction of propagation. The energy and time of the sound particles are recorded at the receiving point, and the energy time distribution at the receiving point can be obtained. In order to improve the accuracy of the energy response at the receiving point, the sound line method has many improved models, such as conical, triangular conical sound beam tracking method.

#### (2) Acoustic image method

The acoustic image method is based on the principle that the mirror reflection path of a reflecting surface can be determined by the location of the mirror sound source and receiving point of that reflecting surface. For a rectangular room, it is intuitively possible to determine all the mirror sources of any reflective order, the acoustic energy at the reception point is the sum of the acoustic energy generated by each image, the distance between each image and the reception point determines the time delay of the reflected sound to the reception point, so that the sequence of the reflected sound can be obtained from the reception point and the position of each image in the acoustic image space. Assuming that the volume of a rectangular room is  $V$ , the number of acoustic images in a sphere with radius  $ct$  is:

$$N_{refl} = \frac{4\pi c^3}{3V} t^3 \quad (1)$$

Equation (1) is suitable in a statistical sense for any form of room. For a hall consisting of  $n$  surfaces, the number of sound images determined by  $i$  reflections is:

$$\begin{aligned} N_{sou} &= \sum_{k=0}^{i-1} n(n-1)^k \\ &= \frac{n}{(n-2)} [(n-1)^i - 1] \approx (n-1)^i \end{aligned} \quad (2)$$

It can be seen that the number of acoustic images increases exponentially with the number of reflections. The acoustic image method spends most of the computational time in determining the validity of the acoustic image, and is therefore only suitable for rooms with simple body shapes or where the number of reflections is sufficiently low.

### II. B. 2) Algorithms for the ODEON software

ODEON software adopts the hybrid method, which absorbs the advantages of the sound-image method and the sound-line method, and at the same time considers the volatility of the sound, and introduces the theoretical model of scattering reflection in the algorithm, so that the simulation results are more comparable with the actual measurement results. In the software algorithm, the simulation is divided into two parts, i.e., the early reflected sound and the late reflected sound part. The direct sound and the early reflected sound contain the intensity, clarity and spatial sense of the sound field, and it is necessary to accurately determine the information of its temporal distribution, direction, etc., which is accurately simulated by the hybrid method of the sound line method and the modified acoustic image method. The simulation of the early reflected sound takes into account the diffraction characteristics arising from the finite scale of the interface as well as the scattering effect of the interface. The later reflections are modeled using a special line-tracking method. A "second source" model is introduced into the algorithm.

In the simulation analysis, according to the complexity of the model, it is necessary to determine a conversion order, which is a key parameter for the prediction of sound quality parameters such as C80, ELEF, and other sound quality parameters that have a high correlation with the early part of the impulse response, etc. The principle of the mixing method used by the ODEON software is shown in Fig. 2.

Track any two neighboring sound lines emitted by a point source  $S$  to the sixth-order reflection, with the conversion order set to 2. The first and second reflections are mirror reflections, and the two sound lines correspond to sound images  $S_1$  and  $S_{12}$ . Reflections higher than the second order produce a secondary source with a directional factor of  $4\cos\theta$  on the reflecting surface, i.e., sound lines higher than the conversion order are randomly distributed in accordance with Lambert's law. Distribution. The treatment of acoustic diffusion in the model introduces a quantitative representation of the scattering coefficient of the acoustic wave at the interface. The scattering coefficient of a given material surface is defined as the ratio of the acoustic energy of the non-specular reflection to the total reflected acoustic energy. This definition applies to incidence at any angle, and the scattering coefficient  $s$  takes values between 0 and 1, with  $s=0$  indicating purely specular reflection and  $s=1$  indicating ideal diffuse reflection. Based on the comparison of computer simulation results with actual measurements, it was found that the scattering coefficient should be taken as 0.1 for large planar surfaces and 0.7 for very irregular surfaces, such as the auditorium area. Theoretically, the scattering coefficient varies with frequency, with scattering due to the finite scale of the surface being reflected more in the low-frequency part and scattering due to the irregularity of the surface being reflected more in the high-frequency part. The question of how to obtain the scattering coefficient at interfaces is still an open one, and in view of this, ISO has set up a working group to develop methods for measuring the scattering coefficient at interfaces.

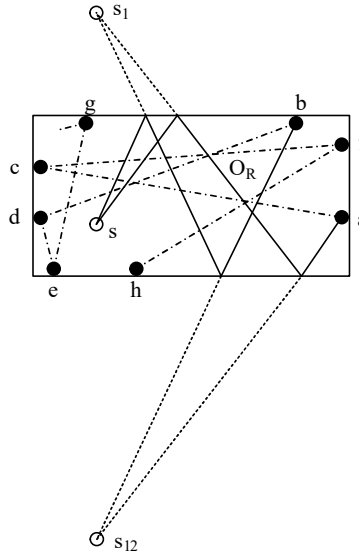


Figure 2: Principle of hybrid method model

### III. Optimization of sound-absorbing material ratios based on topological optimization models

#### III. A. Material interpolation model

Strictly speaking, the topology optimization problem is actually a 0-1 combinatorial planning problem for discrete design variables, i.e., determining the acoustic absorbing material with  $(\rho_e = 1)$  versus without  $(\rho_e = 0)$ . However, the discrete problem is mathematically difficult to solve, so interpolation methods can be used to transform it into a continuous problem for solution:

$$\beta_e = \beta_0 f(\rho_e) \quad (3)$$

where  $\beta_0 = 1$ , denotes the corresponding dielectric conductance when the unit is laid with sound-absorbing material.

In this paper, the most popular SIMP is used, i.e:

$$f(\rho) = \rho^\gamma \quad (4)$$

where  $\gamma$  is the penalty factor, the purpose is to make the intermediate density state quickly approach to the presence of  $(\rho_e = 1)$  and no  $(\rho_e = 0)$ , to avoid the existence of intermediate density units, the previous research shows that  $\gamma=3$  is a more appropriate value.

Although the SIMP method employs a penalty factor to make the intermediate density approximate to 0 or 1, there are still some intermediate density cells in the actual calculation. Here in this paper, based on SIMP, we adopt a penalty function different from the SIMP method, which makes values less than 0.5 approximate to 0, and makes values greater than 0.5 approximate to 1:

$$\Gamma(\rho) = \begin{cases} \rho_{\min} & \rho \leq 0.05 \\ 0.5 + \frac{\arctan[\eta(2\rho-1)]}{2\arctan(\eta)} & 0.05 \leq \rho \leq 0.95 \\ 1 & \rho \geq 0.95 \end{cases} \quad (5)$$

The recommended value of  $\eta$  is 3. If the value is too small, it will not have a penalizing effect, and if the value is too large, the optimal result may not be found.

### III. B. Sensitivity analysis

The objective function is obtained by solving for the design variables:

$$\frac{\partial \Pi}{\partial \rho_e} = 2\Re \left( p_f^* \frac{\partial p_f}{\partial \rho_e} \right) \quad (6)$$

It's available:

$$\frac{\partial p_f}{\partial \rho_e} = G_f \frac{\partial B}{\partial \rho_e} p - [H_f - G_f B] \times [H - GB]^{-1} \left[ G \frac{\partial B}{\partial \rho_e} p \right] \quad (7)$$

After considering the SIMP interpolation function, it can be obtained:

$$\frac{\partial B}{\partial \rho_e} = \frac{\partial B}{\partial \beta_e} \frac{\partial \beta_e}{\partial \rho_e} = \frac{\partial B}{\partial \beta_e} (\gamma \rho_e^{\gamma-1}) \quad (8)$$

The final sensitivity value can be obtained by substituting Eq. (8) into Eq. (7).

### III. C. Iterative update process

Based on the sensitivity analysis, the MMA algorithm is used to solve the above optimization problem. The iterative solution flow of the optimization model is shown in Fig. 3, and the convergence condition is:

$$\left| \frac{\Pi^{k+1} - \Pi^k}{\Pi^k} \right| < \tau \quad (9)$$

where,  $\Pi^k$  is the  $k$  th step objective function;  $\tau$  is the set relative error of convergence.

## IV. Numerical simulation of indoor acoustic environment and improvement of diffusivity

### IV. A. Validation of the two-dimensional boundary element model and the quadratic cosine diffuser approximate boundary model

In this paper, a two-dimensional boundary element model is developed for an apartment as an example. In order to improve the sound diffusivity of the apartment, steps, quadratic cosine diffusers, and porous acoustic materials are installed on the floor, ceiling, and rear wall, respectively. The treated models are represented by models A to N, respectively. When calculating the diffusion gains of the 2D models C to N, the 2D model A was used as the reference model.

In order to obtain a reasonable computational accuracy in a feasible time, the division of boundary cells in this paper adopts the criterion of at least 6 configuration points in one wavelength, i.e., the length of the cell of the constrained quadratic linear segment does not exceed  $\lambda/2$ . In order to verify the calculation results, Morse's simplex formula and the boundary element method are used to solve the two-dimensional models A and B whose boundaries are rigid and soft, respectively, to compare the calculation results.

The frequency response curves of the sound pressure level at the midpoint (5, 2) of the two-dimensional model A calculated by Morse's simplex formula and the boundary element method, respectively, are shown in Fig. 4. From the figure, it can be seen that the computed results of the 2D boundary element model and Morse's simplex formula can be in good agreement in the frequency range under consideration. At most of the frequencies, the two

are almost coincident, and the 2D boundary element model has good accuracy; at a few frequencies such as 40 Hz, the 2D boundary element model has an error of no more than 1 dB.

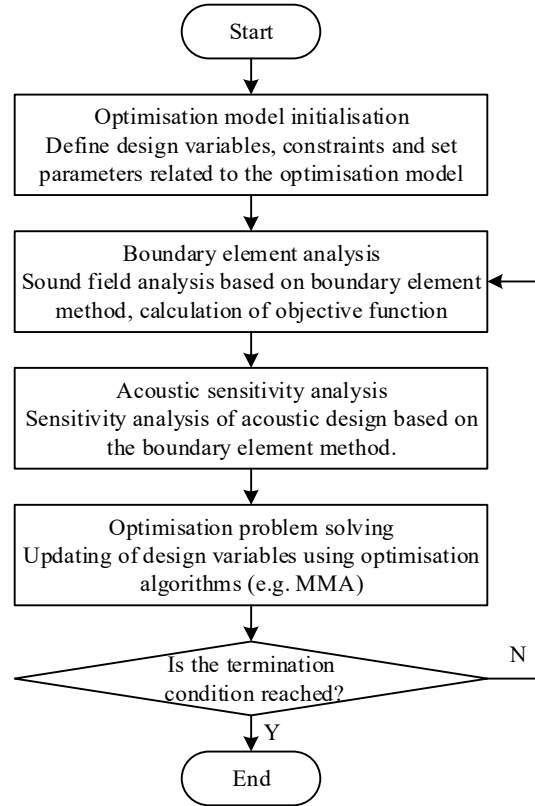


Figure 3: Topology optimization process

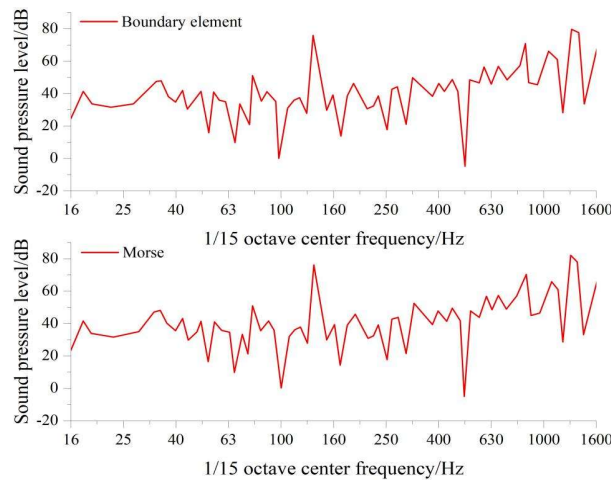


Figure 4: Frequency response curves of the sound pressure level in 2D model A

The frequency response curves of the sound pressure levels at the midpoint (5, 2) of the two-dimensional model  $B$  calculated by Morse's simplex formula and the boundary element method, respectively, are shown in Fig. 5. At 460 Hz and 1520 Hz, the boundary element model has an error of no more than 1 dB; otherwise, the two curves almost completely overlap. Morse's simplex formula is an analytical solution of the Helmholtz equation under the given boundary conditions, and the error in the calculation results of the boundary element method is mainly caused by the boundary discretization and the error of function interpolation. The computational results of the two-



dimensional models  $A$  and  $B$  show that the two-dimensional boundary element method adopted in this paper achieves a more reasonable computational accuracy within a feasible computational time.

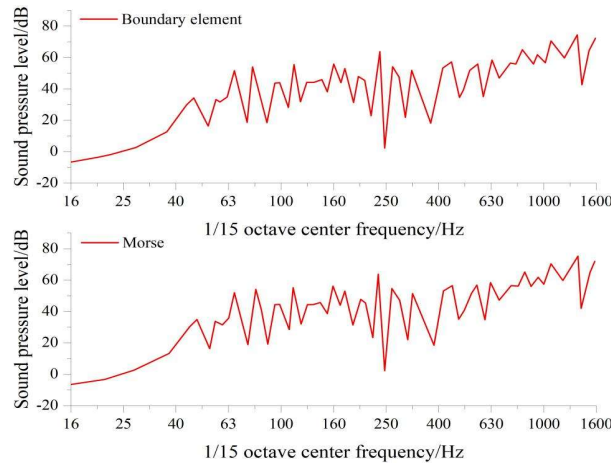


Figure 5: Frequency response curves of the sound pressure level in 2D model B

In the two-dimensional model with a quadratic cosine diffuser, the quadratic cosine diffuser is approximated by the plane of acoustic impedance rate change at the wellhead to simplify the calculation. In order to verify the approximation method, a complete boundary model and an approximate boundary model are built for the two-dimensional model  $C$ , respectively, and the calculation results are compared. In the full boundary model, the thickness of the fins is 0.0035 m. The frequency response curves of the sound pressure levels at the midpoint (5, 2) of the two-dimensional model  $C$  calculated by the full boundary model and the approximate boundary model, respectively, are shown in Fig. 6. The two curves almost completely overlap at frequencies below 205 Hz; at some frequencies above 205 Hz, some deviation between the two curves occurs. Especially at 650 Hz, the error is close to 5 dB, but in most of the frequencies, the deviation of the two curves is not more than 2 dB. On the whole, the trend of the frequency response of the full boundary model can be well reflected by the frequency response curves of the approximate boundary model. In this paper, the acoustic diffusivity of different models is investigated, so the approximate model is used to save a lot of computational time while achieving acceptable prediction results.

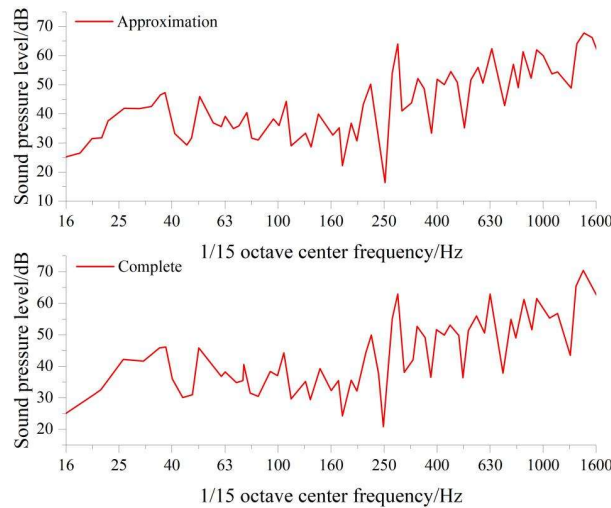


Figure 6: Frequency response curves of the sound pressure level in the 2D model C

#### IV. B. Influence of Acoustic Structures on the Spatial Distribution of Sound Pressure Levels

In this paper, the acoustic diffusion equation interface in the multi-physics field finite element analysis software Comsol Multiphysics is used for numerical simulations. Its acoustic diffusion equation interface can be used to determine the sound pressure level distribution in the coupled space as well as the reverberation time at different locations, and to discretize the continuous space using the finite element method. In Comsol, the size of the grid

dimensions does not depend on the wavelength but on the mean free range. The apartment rooms are modeled in Comsol according to their house type, with the floor heights all set to 4m and the combined openings being the doors of each space. The minimum grid cell size was 0.05m and the maximum was 0.64m, and a total of 60,184 grid cells were created. The volume of the apartment is 250.25m<sup>3</sup>, the surface area is 400.15m<sup>2</sup>, the average free range MFP is 3m, and the largest grid cell size is smaller than the average free range.

By solving the acoustic diffusion equation, the spatial acoustic energy distribution level and the time-containing solution of the acoustic energy flow vector are obtained, and the time step is taken as 0.01s. In order to avoid data duplication, the key time acoustic energy flow direction change is selected. Reverberation time under different working conditions is shown in Fig. 7, when uncoupled, i.e., calculated as the natural reverberation time of each room, the reverberation time of the master bedroom is larger than that of the living room by about 0.3s, which is the reason for the change in the direction of the acoustic energy flow vector. Due to the role of room coupling, the reverberation time of each room is adjusted, which shows that the reverberation time of the master bedroom becomes larger, and the living room and the second bedroom become relatively smaller, and the difference between the reverberation time of the master bedroom and the living room under the same frequency is not more than 0.05s.

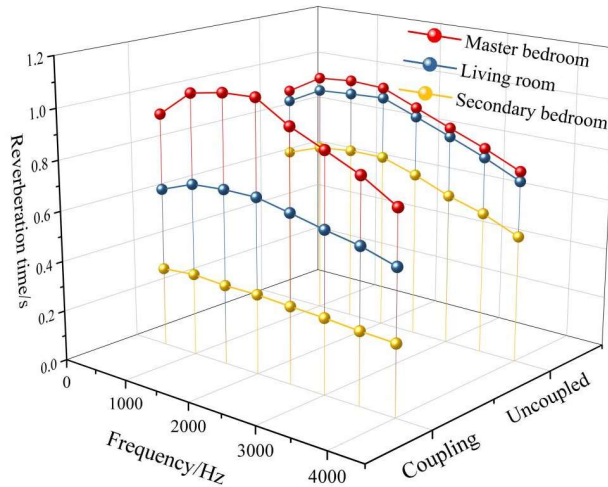


Figure 7: Reverberation time under different working conditions

#### IV. C. Improvement of sound field diffusivity by sound-absorbing materials

The sound absorption coefficient of porous acoustic materials is a function of frequency, which is different at different acoustic frequencies. In order to verify the feasibility of the topology optimization method proposed in this paper, a simplified model of glass fiber acoustic cotton was selected as the optimization object to carry out the study.

In the low-frequency band (less than 300Hz) absorption coefficient is generally low, with the increase in acoustic frequency, the absorption coefficient gradually increases, in the mid-frequency band (300~1000Hz) absorption coefficient with the growth of the frequency of the logarithmic form of growth. Glass fiber acoustic cotton in the frequency band absorption coefficient and trend line shown in Figure 8. 30mm thick glass wool in the mid-frequency band absorption coefficient from 0.146 to 0.614. Acoustic material pore size and high-frequency sound wave wavelength is similar due to the high-frequency sound waves can be made in the air between the air vibration speed up the air and the hole wall of the heat exchange is also accelerated.

Many interconnected tiny pores in the material are the structural characteristics of porous acoustic materials. The solid part of the material (such as glass fibers) in the space formed by the skeleton called tendon tendon makes the material has a certain shape, the pores exist in these tendons between. Fiber thickness determines the density of the material, the finer the fiber, the lower the density of the material, the porosity (material in addition to the closed pore volume outside the pore volume accounted for the percentage of the total volume of the material) will be the greater, the better the acoustic effect.

The initial value of the design variable is set to 1.0, and when the convergence condition is reached, the objective function value is much lower than the corresponding objective function value of the initial design variable, and the volume ratio of the converged material is also lower than 1. The glass fiber acoustic cotton is optimized to obtain the final distribution of acoustic materials after sound barrier optimization. In the process of architectural acoustic design, sound-absorbing material density is a direct indicator of the degree of economy of its materials, when the sound absorption coefficient is determined, the smaller the sound-absorbing panel density, indicating that the more



economical materials. Glass fiber acoustic cotton and optimized material density close to the sound absorption coefficient shown in Figure 9. It can be seen that the optimized material surface density of  $0.39\text{kg/m}^2$  has the largest acoustic absorption coefficient, and also has a good acoustic absorption effect on the mid-frequency band. In order to achieve the same sound absorption effect, the glass fiber acoustic cotton needs a thickness of 80mm to work. The feasibility and effectiveness of the proposed method is verified through the simulation calculation of the optimal design of sound-absorbing material distribution for the two-dimensional sound barrier model.

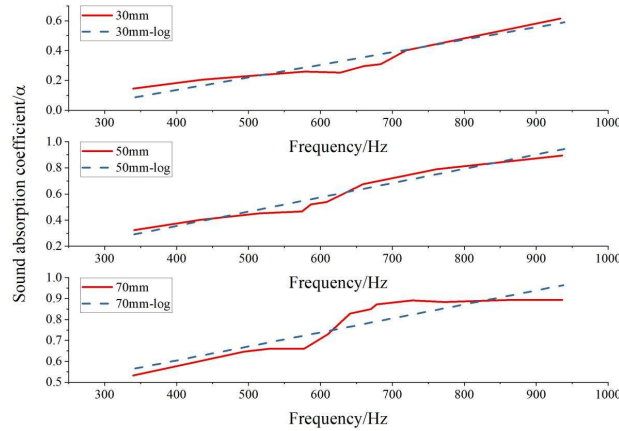


Figure 8: Sound absorption coefficient and trend line in the middle frequency band

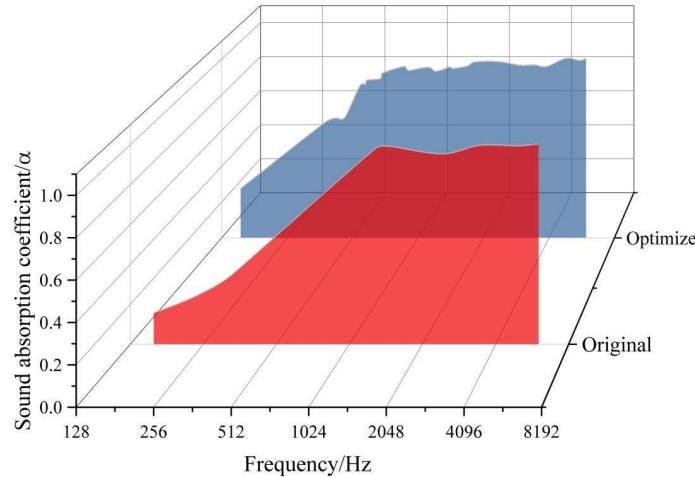


Figure 9: The sound absorption coefficient when the surface density is close

## V. Conclusion

In this study, the acoustic diffusivity of condominiums is investigated using a two-dimensional boundary element model. The two curves of the two-dimensional model C overlap almost completely at frequencies below 205 Hz; at some frequencies above 205 Hz, there is some deviation between the two curves. Especially at 650 Hz, the error is close to 5 dB; nevertheless, at most of the frequencies, the deviation does not exceed 2 dB, demonstrating that the use of the approximate model saves a lot of computational time and at the same time achieves acceptable prediction results. The parameters of the acoustic structure were further varied with the ratio of sound absorbing materials to investigate the effect of these parameters on the diffusivity of the sound field.

(1) When uncoupled, i.e., calculated as the natural reverberation time of each room, the reverberation time of the master bedroom is larger than that of the living room by about 0.3 s, which is the reason for the change in the direction of the acoustic energy flow vector. Due to the role of room coupling, the reverberation time of each room is adjusted, the reverberation time of the master bedroom becomes larger, the living room and the second bedroom is relatively smaller, and the difference between the reverberation time of the master bedroom and the living room is no more than 0.05s under the same frequency.

(2) The surface density of the optimized material is  $0.39\text{kg/m}^2$ , which has the largest sound absorption coefficient and good sound absorption effect in the middle frequency band. In order to achieve the same sound absorption effect, the glass fiber acoustic cotton needs a thickness of 80mm to work. The feasibility and effectiveness of the proposed topology optimization method for sound-absorbing material ratio optimization is verified through the simulation calculation of the optimal design of sound-absorbing material distribution for the two-dimensional sound barrier model.

## References

- [1] Templeton, D., & Saunders, D. (2014). *Acoustic design*. Elsevier.
- [2] Badino, E., Shtrepi, L., & Astolfi, A. (2020, May). Acoustic performance-based design: a brief overview of the opportunities and limits in current practice. In *Acoustics* (Vol. 2, No. 2, pp. 246-278). mdpi.
- [3] Chen, K., Kang, J., & Ma, H. (2023). Evaluation of healthy indoor acoustic environments in residential buildings by the occupants: A mixed-method approach. *Building and Environment*, 246, 110950.
- [4] Dokmeci Yorukoglu, P. N., & Kang, J. (2016). Analysing sound environment and architectural characteristics of libraries through indoor soundscape framework. *Archives of acoustics*, 41(2), 203-212.
- [5] Russo, D., & Ruggiero, A. (2019). Choice of the optimal acoustic design of a school classroom and experimental verification. *Applied Acoustics*, 146, 280-287.
- [6] Kang, S., Mak, C. M., Ou, D., & Zhang, Y. (2022). An investigation of acoustic environments in large and medium-sized open-plan offices in China. *Applied Acoustics*, 186, 108447.
- [7] Hossain, M. R., Manohare, M., & King, E. A. (2025). Systematic review of indoor soundscape assessments: Activity-based psycho-acoustics analysis. *Building Acoustics*, 32(1), 123-141.
- [8] Aletta, F., & Kang, J. (2019). Promoting healthy and supportive acoustic environments: Going beyond the quietness. *International journal of environmental research and public health*, 16(24), 4988.
- [9] Chen, K., Kang, J., & Ma, H. (2024). Effects of sound-source characteristics and personal factors on the perceived controllability of indoor acoustic environments in high-rise multi-unit residences. *Building and Environment*, 264, 111935.
- [10] Mohamed, A. S. A., Ibrahim, A. H., & Rahman, D. A. (2024). The Impact of Material Selection on Acoustic Performance in Interior Design: A Scientific Investigation. *Journal of Art, Design and Music*, 3(2), 12.
- [11] Amran, M., Fediuk, R., Murali, G., Vatin, N., & Al-Fakih, A. (2021). Sound-absorbing acoustic concretes: A review. *Sustainability*, 13(19), 10712.
- [12] Cucharero, J., Hänninen, T., & Lokki, T. (2019, August). Influence of sound-absorbing material placement on room acoustical parameters. In *Acoustics* (Vol. 1, No. 3, pp. 644-660). MDPI.
- [13] ZAHARIA, M. C., DOBRE, D., & DRAGOMIR, C. S. (2024). ACOUSTIC ABSORPTION CHARACTERISTICS THAT ARE USED IN THE ACOUSTIC DESIGN OF INTERIORS-COMPARISONS BETWEEN SOME CLASSICAL MATERIALS AND NATURAL, ECOLOGICAL MATERIALS. *Scientific Papers. Series E. Land Reclamation, Earth Observation & Surveying, Environmental Engineering*, 13.
- [14] Kalauni, K., & Pawar, S. J. (2019). A review on the taxonomy, factors associated with sound absorption and theoretical modeling of porous sound absorbing materials. *Journal of Porous Materials*, 26(6), 1795-1819.
- [15] Jo, H. I., & Jeon, J. Y. (2020). Effect of the appropriateness of sound environment on urban soundscape assessment. *Building and environment*, 179, 106975.
- [16] Yang, D., & Mak, C. M. (2017). An assessment model of classroom acoustical environment based on fuzzy comprehensive evaluation method. *Applied acoustics*, 127, 292-296.
- [17] Mao, M., Wu, F., Hu, S., Dai, X., He, Q., Tang, J., & Hong, X. (2024). Analysis and Optimization of the Noise Reduction Performance of Sound-Absorbing Materials in Complex Environments. *Processes*, 12(11), 2582.